




QCD sum-rule determination of the axial-vector mixing angle in the $B_c(1P)$ sector

T. M. Aliev ^{1,*} S. Bilmis ^{1,2,†} and M. Savci ^{1,‡}

¹*Department of Physics, Middle East Technical University, Ankara, 06800, Turkey*

²*TUBITAK ULAKBIM, Ankara, 06510, Turkey*

(Dated: July 2, 2026)

Abstract

We determine the mixing angle between the 1^1P_1 and 1^3P_1 axial-vector states in the $B_c(1P)$ sector using QCD sum rules. The analysis gives $\theta_{B_c(1P)} = (43.3 \pm 0.2)^\circ$, indicating sizable mixing between these two states. We also compare our result with theoretical studies available in the literature.

arXiv:2607.00593v1 [hep-ph] 1 Jul 2026

* taliev@metu.edu.tr

† sbilmis@metu.edu.tr

‡ savci@metu.edu.tr

I. INTRODUCTION

The spectroscopy of heavy hadrons provides an important testing ground for our understanding of the nonperturbative regime of quantum chromodynamics (QCD). Among these systems, the B_c meson family occupies a special position. In contrast to charmonium and bottomonium, the B_c mesons are composed of two heavy quarks with different flavors, $\bar{b}c$. This asymmetric heavy-heavy structure makes the B_c spectrum richer than ordinary quarkonium systems and provides a complementary laboratory for studying the dynamics of heavy quarks inside hadrons. Since both constituent quark masses are much larger than the QCD scale, the B_c system is also well suited for comparisons among lattice QCD, quark models, nonrelativistic QCD, and QCD sum-rule calculations [1–4].

Experimentally, the ground-state B_c meson was first observed by the CDF Collaboration at the Tevatron [5, 6]. Since then, significant progress has been achieved in the study of its excited spectrum. The first evidence for an excited B_c state was reported by the ATLAS Collaboration [7], and the $2S$ sector was subsequently resolved by the CMS and LHCb Collaborations [8, 9]. The ATLAS Collaboration has also recently reported the observation of a new state in the $B_c^+\gamma$ channel, consistent with the lowest vector B_c^{*+} state [10]. More directly relevant for the present work, the LHCb Collaboration recently reported the observation of orbitally excited B_c^+ structures in the $B_c^+\gamma$ mass spectrum [11, 12]. These structures are compatible with the lowest P -wave B_c^+ states and provide new experimental motivation for refined theoretical studies of the $B_c(1P)$ sector.

The $1P$ B_c multiplet contains four states: the spin-singlet 1^1P_1 configuration and the spin-triplet 1^3P_0 , 1^3P_1 , and 1^3P_2 configurations. Since the B_c meson is composed of two different heavy flavors, charge conjugation is not a good quantum number. Consequently, the two axial-vector configurations 1^1P_1 and 1^3P_1 can mix and form the physical $J^P = 1^+$ axial-vector states. In the following we use the notation $B_c(1P)$ to specify the theoretical sector under study; the individual quantum-number assignments of the experimentally observed structures have not yet been fully resolved. Following the convention used in Ref. [12],

$$\begin{pmatrix} |1P_1'\rangle \\ |1P_1\rangle \end{pmatrix} = \begin{pmatrix} \cos\theta & \sin\theta \\ -\sin\theta & \cos\theta \end{pmatrix} \begin{pmatrix} |1^1P_1\rangle \\ |1^3P_1\rangle \end{pmatrix},$$

the parameter θ denotes the $1^1P_1 - 1^3P_1$ mixing angle. This mixing is not merely a formal property of the spectrum. It affects the identification of the physical $B_c(1P)$ states, their radiative transition patterns, the relative contributions of the different P -wave states to the observed $B_c^+\gamma$ spectrum, and the branching ratios used in theory-constrained experimental analyses [12].

Several theoretical approaches have been used to study the B_c spectrum, including lattice QCD,

nonrelativistic and relativistic quark models, Bethe–Salpeter approaches, Dyson–Schwinger methods, coupled-channel models, and QCD sum rules [1, 3, 4, 13–22]. These studies generally predict the $B_c(1P)$ masses in the region now probed experimentally. In those analyses where the axial-vector mixing is discussed, the predicted $1^1P_1 - 1^3P_1$ mixing angle shows a sizable model dependence. For example, the theory-constrained analysis of the LHCb $B_c^+\gamma$ spectrum compares predictions in which the mixing angle ranges from values near 20° to values above 50° , depending on the model input [12]. This spread indicates that an independent determination of the $B_c(1P)$ axial-vector mixing angle is useful for both spectroscopy and phenomenological applications.

QCD sum rules provide a complementary nonperturbative framework for relating hadronic observables to QCD degrees of freedom. In our previous work, this method was applied to the $1^3P_1 - 1^1P_1$ mixing angles of heavy axial-vector mesons containing one heavy and one light quark [23]. The $B_c(1P)$ system requires a separate analysis because it contains two heavy quarks with different flavors.

In the present work, we determine the $1^1P_1 - 1^3P_1$ mixing angle of the axial-vector $B_c(1P)$ states within the QCD sum-rule approach. Our aim is to provide an independent estimation of this quantity and to assess its relevance for the interpretation of the recently observed $B_c(1P)$ structures.

The paper is organized as follows. In Sec. II, we introduce the interpolating currents, define the correlation functions, and derive the QCD sum rule for the mixing angle. In Sec. III, we present the numerical analysis of the obtained sum rule and extract the value of the mixing angle. In this section, we also compare our result with existing theoretical predictions. The final section is devoted to our conclusions.

II. THEORETICAL FRAMEWORK

In this section, we derive the QCD sum rule for the mixing angle between the 1^1P_1 and 1^3P_1 axial-vector $B_c(1P)$ states. We first introduce the interpolating currents and the corresponding two-point correlation functions. The correlation functions are represented both at the hadronic level, in terms of physical intermediate states, and at the QCD level, in the deep Euclidean region $p^2 \ll (m_b + m_c)^2$, using the operator product expansion. Equating these two representations after Borel transformation and continuum subtraction yields the desired sum rule.

We use the quark-content convention $B_c^+ = \bar{b}c$. The two interpolating currents employed for the axial-vector $B_c(1P)$ system are chosen as

$$J_\mu^A(x) = \bar{b}(x)\gamma_\mu\gamma_5c(x), \quad (1)$$

$$J_\mu^B(x) = i \bar{b}(x) \sigma_{\mu\alpha} \frac{p^\alpha}{m_b + m_c} \gamma_5 c(x), \quad (2)$$

where

$$\sigma_{\mu\nu} = \frac{i}{2} [\gamma_\mu, \gamma_\nu]. \quad (3)$$

The factor $1/(m_b + m_c)$ in J_μ^B is introduced so that the two currents have the same mass dimension. The corresponding two-point correlation functions are

$$\Pi_{\mu\nu}^{ij}(p) = i \int d^4x e^{ip \cdot x} \langle 0 | T \{ J_\mu^i(x) J_\nu^{j\dagger}(0) \} | 0 \rangle, \quad i, j = A, B. \quad (4)$$

They are decomposed as

$$\Pi_{\mu\nu}^{ij}(p) = \left(-g_{\mu\nu} + \frac{p_\mu p_\nu}{p^2} \right) \Pi_1^{ij}(p^2) + \frac{p_\mu p_\nu}{p^2} \Pi_0^{ij}(p^2), \quad (5)$$

where the transverse amplitude Π_1^{ij} contains the spin-one contribution. We project it using

$$\Pi_1^{ij}(p^2) = \frac{1}{3} \left(g^{\mu\nu} - \frac{p^\mu p^\nu}{p^2} \right) \Pi_{\mu\nu}^{ij}(p). \quad (6)$$

The physical axial-vector currents are obtained by rotating the current basis,

$$\begin{pmatrix} J_\mu^{(1)} \\ J_\mu^{(2)} \end{pmatrix} = \begin{pmatrix} \cos \theta & -\sin \theta \\ \sin \theta & \cos \theta \end{pmatrix} \begin{pmatrix} J_\mu^A \\ J_\mu^B \end{pmatrix}. \quad (7)$$

The mixing angle is fixed by requiring that the nondiagonal correlation function vanish in the physical basis. Hence,

$$\Pi_1^{AB}(p^2) \cos 2\theta + \frac{1}{2} [\Pi_1^{AA}(p^2) - \Pi_1^{BB}(p^2)] \sin 2\theta = 0. \quad (8)$$

After Borel transformation and continuum subtraction, the sum rule for the mixing angle becomes

$$\tan 2\theta = -\frac{2\Pi_1^{AB}(M^2, s_0)}{\Pi_1^{AA}(M^2, s_0) - \Pi_1^{BB}(M^2, s_0)}, \quad (9)$$

where M^2 is the Borel parameter and s_0 is the continuum threshold.

The QCD side is calculated in the deep Euclidean region using the operator product expansion. After applying Wick's theorem to the corresponding correlation functions, we obtain

$$\Pi_{\mu\nu}^{AA}(p) = -i \int \frac{d^4k}{(2\pi)^4} \text{Tr} [\gamma_\mu \gamma_5 S_c(k) \gamma_\nu \gamma_5 S_b(k-p)], \quad (10)$$

$$\Pi_{\mu\nu}^{AB}(p) = -i \int \frac{d^4k}{(2\pi)^4} \text{Tr} \left[\gamma_\mu \gamma_5 S_c(k) i\sigma_{\nu\alpha} \frac{p^\alpha}{m_b + m_c} \gamma_5 S_b(k-p) \right], \quad (11)$$

$$\Pi_{\mu\nu}^{BB}(p) = -i \int \frac{d^4k}{(2\pi)^4} \text{Tr} \left[i\sigma_{\mu\alpha} \frac{p^\alpha}{m_b + m_c} \gamma_5 S_c(k) i\sigma_{\nu\beta} \frac{p^\beta}{m_b + m_c} \gamma_5 S_b(k-p) \right]. \quad (12)$$

Here the trace is taken over Dirac and color indices. The algebraic manipulations of the Dirac matrices, Lorentz structures, and color factors were performed with FEYNCALC [24–26]. In our calculations, we use the fixed-point gauge,

$$x^\mu A_\mu(x) = 0, \quad (13)$$

in which the gauge potential can be expressed in terms of the field-strength tensor as

$$A_\mu(x) = \int_0^1 dt t x^\nu G_{\nu\mu}(tx) = \frac{1}{2} x^\nu G_{\nu\mu}(0) + \frac{1}{3} x^\alpha x^\nu D_\alpha G_{\nu\mu}(0) + \dots \quad (14)$$

The massive-quark propagator, including the one-gluon, two-gluon, and three-gluon background-field contributions, can be written in momentum space as follows:

$$S_Q(k) = S_Q^{(0)}(k) + S_Q^{(G)}(k) + S_Q^{(GG)}(k) + S_Q^{(GGG)}(k) + \dots, \quad Q = b, c, \quad (15)$$

where the notation follows the standard background-field expansion [27–31]. Explicitly, the free and one-gluon parts of the heavy-quark propagator are

$$S_Q^{(0)}(k) = \frac{\not{k} + m_Q}{k^2 - m_Q^2}, \quad (16)$$

and

$$S_Q^{(G)}(k) = -\frac{g_s G_{\alpha\beta}^A T^A}{4} \frac{\sigma^{\alpha\beta}(\not{k} + m_Q) + (\not{k} + m_Q)\sigma^{\alpha\beta}}{(k^2 - m_Q^2)^2}. \quad (17)$$

The two-gluon term of the propagator can be expressed as follows [29, 31]:

$$S_Q^{(GG)}(k) = -\frac{g_s^2}{4} G_{\mu\rho}^A G_{\nu\sigma}^B T^A T^B \frac{\not{k} + m_Q}{(k^2 - m_Q^2)^5} (f^{\mu\rho\nu\sigma} + f^{\mu\nu\rho\sigma} + f^{\mu\nu\sigma\rho}), \quad (18)$$

while the three-gluon term is

$$\begin{aligned} S_Q^{(GGG)}(k) &= \frac{g_s^3}{8} G_{\mu\alpha}^A G_{\nu\beta}^B G_{\rho\gamma}^C T^A T^B T^C \frac{\not{k} + m_Q}{(k^2 - m_Q^2)^7} \\ &\quad \times \left(f^{\mu\alpha\nu\beta\rho\gamma} + f^{\mu\alpha\nu\rho\beta\gamma} + f^{\mu\alpha\nu\rho\gamma\beta} + f^{\mu\nu\alpha\beta\rho\gamma} + f^{\mu\nu\beta\alpha\rho\gamma} + f^{\mu\nu\beta\rho\alpha\gamma} \right) \end{aligned}$$

$$\begin{aligned}
& + f^{\mu\nu\beta\rho\gamma\alpha} + f^{\mu\nu\alpha\rho\beta\gamma} + f^{\mu\nu\alpha\rho\gamma\beta} + f^{\mu\nu\rho\alpha\beta\gamma} + f^{\mu\nu\rho\beta\alpha\gamma} + f^{\mu\nu\rho\beta\gamma\alpha} \\
& + f^{\mu\nu\rho\alpha\gamma\beta} + f^{\mu\nu\rho\gamma\alpha\beta} + f^{\mu\nu\rho\gamma\beta\alpha}).
\end{aligned} \tag{19}$$

The shorthand f denotes the ordered Dirac string

$$f^{\mu\nu\cdots\alpha\beta} = \gamma^\mu(\not{k} + m_Q)\gamma^\nu(\not{k} + m_Q)\cdots\gamma^\alpha(\not{k} + m_Q)\gamma^\beta(\not{k} + m_Q). \tag{20}$$

In these expressions, $T^A = \lambda^A/2$, where λ^A are the Gell-Mann matrices in color space, and A, B, C label color-adjoint indices.

After vacuum averaging, these propagator terms generate the perturbative, two-gluon-condensate and three-gluon-condensate parts of the invariant amplitudes.

After performing Borel transformation, the projected amplitudes can be written as

$$\Pi_1^{ij}(M^2, s_0) = \Pi_{1,\text{pert}}^{ij}(M^2, s_0) + \Pi_{1,\langle G^2 \rangle}^{ij}(M^2, s_0) + \Pi_{1,\langle G^3 \rangle}^{ij}(M^2, s_0), \quad i, j = A, B. \tag{21}$$

The perturbative contribution is represented by the dispersion integral

$$\Pi_{1,\text{pert}}^{ij}(M^2, s_0) = \int_{(m_b+m_c)^2}^{s_0} ds \rho_{\text{pert}}^{ij}(s) e^{-s/M^2}, \tag{22}$$

where $\rho_{\text{pert}}^{ij}(s)$ are the spectral densities of the corresponding correlation functions. They are obtained as

$$\rho_{\text{pert}}^{AA}(s) = -\frac{3}{8\pi^2 s^2} [(m_b + m_c)^2 - s] [(m_b - m_c)^2 + 2s] \sqrt{\lambda(s, m_b, m_c)}, \tag{23}$$

$$\rho_{\text{pert}}^{AB}(s) = \frac{9}{8\pi^2 s(m_b + m_c)} (m_b - m_c) [(m_b + m_c)^2 - s] \sqrt{\lambda(s, m_b, m_c)}, \tag{24}$$

$$\rho_{\text{pert}}^{BB}(s) = \frac{3}{8\pi^2 s(m_b + m_c)^2} \left[-2(m_b^2 - m_c^2)^2 + (m_b^2 - 6m_b m_c + m_c^2)s + s^2 \right] \sqrt{\lambda(s, m_b, m_c)} \tag{25}$$

where

$$\lambda(s, m_b, m_c) = s^2 + m_b^4 + m_c^4 - 2sm_b^2 - 2sm_c^2 - 2m_b^2 m_c^2. \tag{26}$$

The condensate terms are obtained by Feynman parametrizing the corresponding background-field contributions and applying the Borel transformation directly. Introducing

$$\bar{s}(x) = \frac{m_c^2 x + m_b^2(1-x)}{x(1-x)}, \tag{27}$$

TABLE I: Input parameters used in the numerical analysis.

Parameter	Value	Reference
$m_b(m_b)$	(4.18 ± 0.03) GeV	[32]
$m_c(m_c)$	(1.27 ± 0.02) GeV	[32]
$\langle \alpha_s G^2 \rangle$	$(6.49 \pm 0.35) \times 10^{-2}$ GeV ⁴	[33]
$\langle g_s^3 G^3 \rangle$	(8.2 ± 1.0) GeV ² $\langle \alpha_s G^2 \rangle$	[33]

the continuum subtraction restricts the integration region to

$$x_- \leq x \leq x_+, \quad x_{\pm} = \frac{s_0 + m_b^2 - m_c^2 \pm \sqrt{\lambda(s_0, m_b, m_c)}}{2s_0}, \quad (28)$$

For terms of the form $(Q^2 + \bar{s})^{-n}$, the Borel transformation gives

$$\mathcal{B}_{M^2} \left[\frac{1}{(Q^2 + \bar{s})^n} \right] = \frac{1}{(n-1)! (M^2)^{n-1}} e^{-\bar{s}/M^2}. \quad (29)$$

Thus the condensate contributions can be written schematically as

$$\Pi_{1,(Gr)}^{ij}(M^2, s_0) = \int_{x_-}^{x_+} dx e^{-\bar{s}(x)/M^2} \sum_n \frac{C_{n,r}^{ij}(x)}{(n-1)! (M^2)^{n-1}}, \quad r = 2, 3. \quad (30)$$

The coefficient functions $C_{n,r}^{ij}(x)$, including the corresponding condensate factors for $r = 2, 3$, are obtained from the color and Dirac traces of the background-field propagator contributions after applying the spin-one projection. Since the explicit expressions are rather lengthy, they are not displayed here but are available from the authors upon request. Substituting Eq. (21) into Eq. (9) gives the final sum rule used in the numerical analysis.

III. NUMERICAL ANALYSIS

In this section we present the numerical analysis of the sum rule in Eq. (9). The mixing angle is evaluated as a function of the Borel parameter M^2 and the continuum threshold s_0 . These auxiliary parameters are varied in a region where the extracted angle shows a stable behavior, and the uncertainty is estimated by varying both the QCD input parameters and the sum-rule parameters within the adopted ranges.

The input parameters used in the numerical analysis, together with their references, are listed in Table I. The heavy-quark masses are quoted in the $\overline{\text{MS}}$ scheme.

For each point in the (M^2, s_0) plane, the invariant amplitudes Π_1^{AA} , Π_1^{AB} , and Π_1^{BB} are evaluated

from Eq. (21) and substituted into Eq. (9). Since the angle is determined through $\tan 2\theta$, the branch of the arctangent is chosen continuously in the physical region relevant for the $B_c(1P)$ axial-vector states. The sum rule contains a ratio of invariant amplitudes; therefore part of the common normalization uncertainty cancels in the extraction of the angle.

The Borel parameter and continuum threshold must be chosen in a region where the sum-rule prediction is reliable. We follow the standard QCD sum-rule criteria: the lower limit of M^2 is fixed by the convergence of the operator product expansion, while the upper limit is fixed by requiring that the lowest-state contribution is not dominated by the continuum. The threshold s_0 is chosen above the squared mass region of the lowest P -wave B_c states and varied around this value to estimate the residual continuum-threshold dependence. The numerical window is also consistent with the range used in the QCD sum-rule analysis of vector and axial-vector B_c mesons in Ref. [22]. In the present analysis we use

$$7 \text{ GeV}^2 \leq M^2 \leq 9 \text{ GeV}^2, \quad 53 \text{ GeV}^2 \leq s_0 \leq 55 \text{ GeV}^2. \quad (31)$$

In Fig. 1, we present the dependence of the mixing angle on M^2 at $s_0 = 53 \text{ GeV}^2$. From this figure we deduce that the perturbative contribution gives the main part of the result, while adding the two-gluon and three-gluon condensate terms produces only a tiny shift in the extracted angle.

In the chosen window the physical result should be almost independent of the auxiliary parameters. This stability is checked explicitly in Fig. 2. The upper panel shows the dependence of the mixing angle on M^2 for fixed values of s_0 , while the lower panel shows the dependence on s_0 for fixed values of M^2 . In both cases, the extracted angle changes only weakly in the selected working region.

To estimate the uncertainty, we perform a Monte Carlo sampling of the input parameters in Table I together with the auxiliary parameters in Eq. (31). For each randomly generated point, the Borel-transformed amplitudes are evaluated and the mixing angle is extracted from Eq. (9). The resulting distribution is shown in Fig. 3. We fit this distribution with a Gaussian and take the mean value and one-standard-deviation width as the central value and the 1σ uncertainty.

This procedure gives

$$\theta_{B_c(1P)} = (43.3 \pm 0.2)^\circ. \quad (32)$$

The quoted uncertainty includes the variation of the Borel parameter, continuum threshold, heavy-quark masses, and gluon-condensate inputs. This value indicates a sizable mixing between the 1^1P_1 and 1^3P_1 components of the physical $B_c(1P)$ axial-vector states. In other words, the physical 1^+ states are expected to be strong mixtures of the two axial-vector configurations rather than nearly pure 1^1P_1 or 1^3P_1 states.

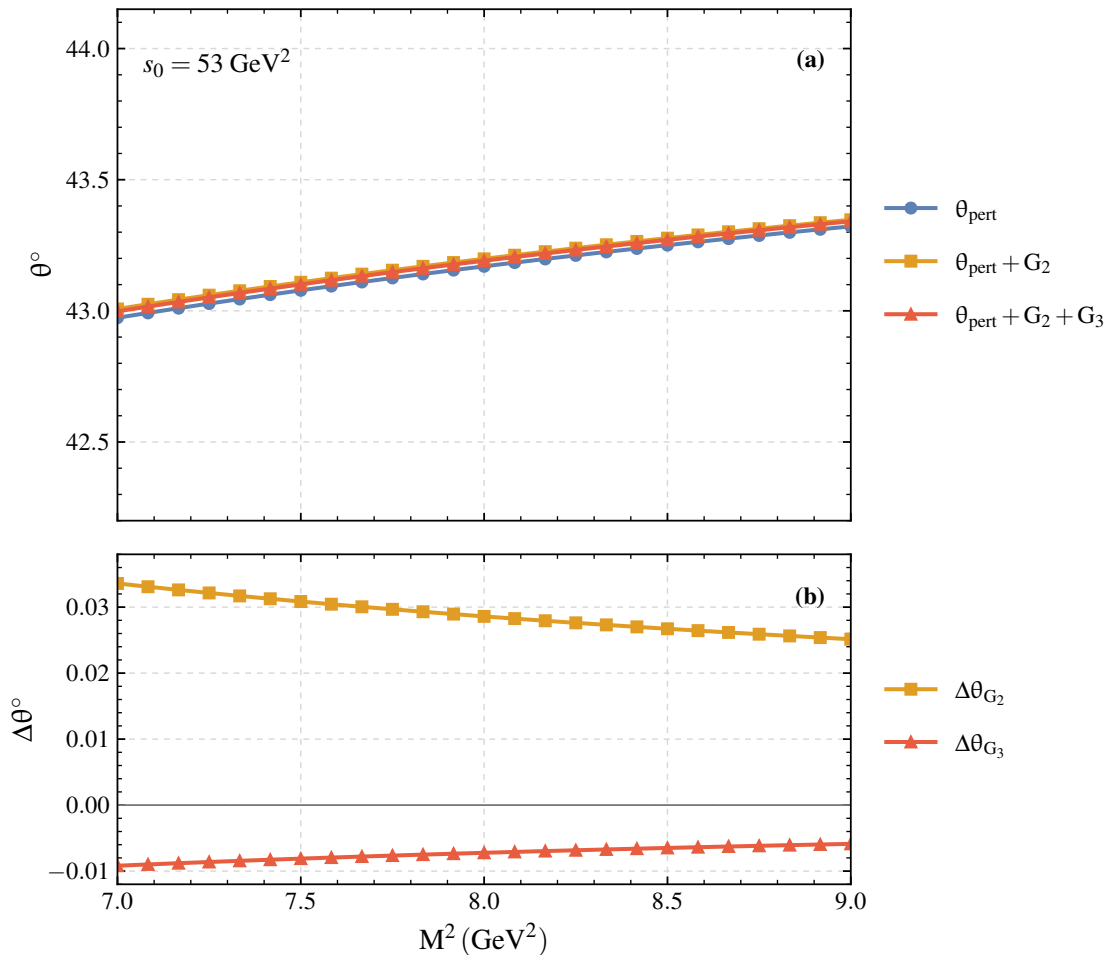


FIG. 1: Borel-mass dependence of the mixing angle at $s_0 = 53 \text{ GeV}^2$. Panel (a) shows the perturbative result and the successive inclusion of the dimension-four and dimension-six gluon-condensate contributions. Panel (b) displays the corresponding incremental shifts, $\Delta\theta_{G_2} = \theta_{\text{pert}+G_2} - \theta_{\text{pert}}$ and $\Delta\theta_{G_3} = \theta_{\text{pert}+G_2+G_3} - \theta_{\text{pert}+G_2}$.

A final comment on the uncertainty is in order. The calculations presented in this work is done on leading-order. Perturbative α_s corrections to the heavy-heavy correlators are not included. Since the mixing angle is determined from a ratio of correlation functions, a radiative correction common to the relevant channels would largely cancel. However, this cancellation need not be exact, because channel-dependent corrections to Π_1^{AA} , Π_1^{AB} , and Π_1^{BB} may still shift the extracted angle. Recent QCD sum-rule analyses of B_c -meson decay constants have included next-to-leading-order corrections to the perturbative contribution, illustrating that such radiative effects are relevant in precision studies of heavy-heavy correlators [34]. A dedicated calculation of the corresponding NLO corrections for the present mixed axial-vector channels would therefore be required for a fully systematic uncertainty estimation.

The $B_c(1P)$ axial-vector mixing angle has been studied in several theoretical approaches. A comparison of representative results is given in Table II. The predictions show a sizable model

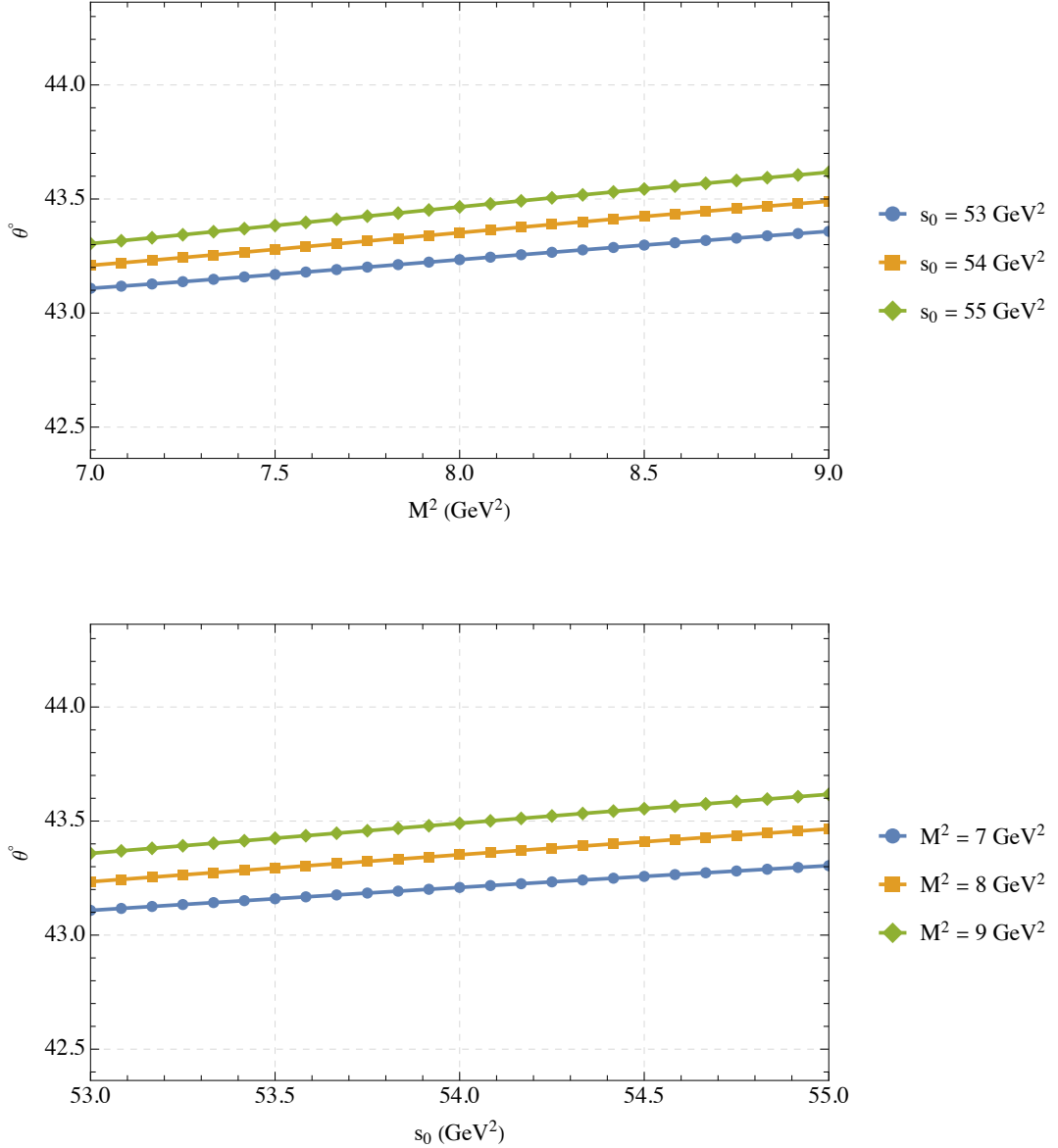


FIG. 2: Dependence of the extracted $B_c(1P)$ axial-vector mixing angle on the auxiliary parameters in the selected sum-rule window. Upper panel: dependence on the Borel parameter M^2 for different fixed values of the continuum threshold s_0 . Lower panel: dependence on s_0 for different fixed values of M^2 .

dependence. Most positive values lie in the range $17^\circ - 36^\circ$, while some analyses give larger or convention-dependent results, extending up to about 55° . Our QCD sum-rule result lies within the broad spectrum of existing theoretical predictions.

The phenomenological importance of this angle is enhanced by the recent LHCb observation of a broad peaking structure compatible with the lowest $B_c(1P)^+$ multiplet in the $B_c^+ \gamma$ spectrum [11, 12]. Since the individual contributions from the members of the $1P$ multiplet have not yet been resolved, theoretical information on the masses, radiative transition patterns, and axial-vector mixing angle is

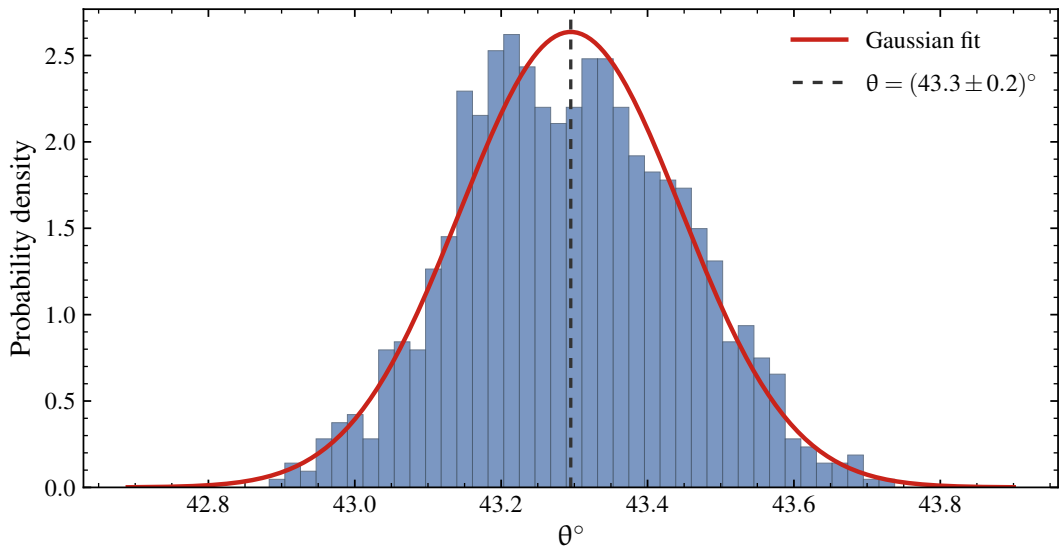


FIG. 3: Monte Carlo distribution of the extracted $B_c(1P)$ axial-vector mixing angle obtained by varying the input parameters, M^2 , and s_0 within the adopted ranges.

TABLE II: Comparison of the $1^1P_1 - 1^3P_1$ mixing angle of the $B_c(1P)$ axial-vector states obtained in different theoretical approaches. The values quoted from the literature follow the convention used in the corresponding references.

Method / Model	θ
Lattice QCD [1]	33.4°
Potential model [13]	17.1°
QCD potential model [14]	25.6°
Phenomenological model [15]	28.5°
Relativistic quark model [16]	20.4°
Relativized quark model [3]	22.4°
Quark model [4]	18.7°
Nonrelativistic quark model [17]	35.5°
Bethe-Salpeter approach [18]	32.2°
Modified Godfrey-Isgur model [19]	-24.3°
Spectroscopic survey [20]	35.2°
Coupled-channel model [21]	55.0°
QCD sum rules (This work)	$(43.3 \pm 0.2)^\circ$

important for assigning the observed structures and for constructing theory-constrained fit models. The mixing angle enters the radiative transition amplitudes of the axial-vector states and can affect the relative contributions of the different P -wave states to the observed $B_c^+\gamma$ signal. As larger data samples and more detailed studies of the excited beauty-charm spectrum become available, independent nonperturbative inputs such as the present QCD sum-rule determination can help constrain phenomenological models and guide future interpretations of the $B_c(1P)$ sector.

IV. CONCLUSION

We have determined the $1^1P_1 - 1^3P_1$ mixing angle in the $B_c(1P)$ axial-vector sector using QCD sum rules. The analysis was based on two-point correlation functions constructed from axial-vector and tensor interpolating currents and evaluated using the operator product expansion. Perturbative, two-gluon-condensate, and three-gluon-condensate contributions were included.

After Borel transformation and continuum subtraction, the mixing angle was extracted from the diagonalization condition of the projected spin-one correlation matrix. The final result is

$$\theta_{B_c(1P)} = (43.3 \pm 0.2)^\circ. \quad (33)$$

This value indicates a sizable mixing of the two axial-vector configurations 1^1P_1 and 1^3P_1 . We also perform comparison of our results with existing theoretical predictions on the mixing angle.

The result provides complementary theoretical input for studies of the recently observed orbitally excited B_c^+ structures in the $B_c^+\gamma$ spectrum. As future experimental analyses further resolve the $B_c(1P)$ multiplet, the mixing angle can be used in phenomenological studies of radiative transitions and in theory-constrained descriptions of the excited beauty-charm spectrum.

ACKNOWLEDGMENTS

We thank N. Gubernari for useful correspondence regarding NLO corrections for B_c systems.

-
- [1] C. T. H. Davies, K. Hornbostel, G. P. Lepage, A. J. Lidsey, J. Shigemitsu, and J. Sloan, “*B_c spectroscopy from lattice QCD*,” Phys. Lett. B **382** (1996) 131–137, [[hep-lat/9602020](#)].
 - [2] N. Mathur, M. Padmanath, and S. Mondal, “*Precise predictions of charmed-bottom hadrons from lattice QCD*,” Phys. Rev. Lett. **121** no. 20, (2018) 202002, [[1806.04151](#)].
 - [3] S. Godfrey, “*Spectroscopy of B_c mesons in the relativized quark model*,” Phys. Rev. D **70** (2004) 054017, [[hep-ph/0406228](#)].
 - [4] E. J. Eichten and C. Quigg, “*Mesons with Beauty and Charm: New Horizons in Spectroscopy*,” Phys. Rev. D **99** no. 5, (2019) 054025, [[1902.09735](#)].
 - [5] **CDF** Collaboration, F. Abe *et al.*, “*Observation of the B_c meson in p \bar{p} collisions at $\sqrt{s} = 1.8$ TeV*,” Phys. Rev. Lett. **81** (1998) 2432–2437, [[hep-ex/9805034](#)].

- [6] **CDF** Collaboration, F. Abe *et al.*, “*Observation of B_c mesons in $p\bar{p}$ collisions at $\sqrt{s} = 1.8$ TeV,*” Phys. Rev. D **58** (1998) 112004, [hep-ex/9804014].
- [7] **ATLAS** Collaboration, G. Aad *et al.*, “*Observation of an Excited B_c^\pm Meson State with the ATLAS Detector,*” Phys. Rev. Lett. **113** no. 21, (2014) 212004, [1407.1032].
- [8] **CMS** Collaboration, A. M. Sirunyan *et al.*, “*Observation of Two Excited B_c^+ States and Measurement of the $B_c^+(2S)$ Mass in pp Collisions at $\sqrt{s} = 13$ TeV,*” Phys. Rev. Lett. **122** no. 13, (2019) 132001, [1902.00571].
- [9] **LHCb** Collaboration, R. Aaij *et al.*, “*Observation of an excited B_c^+ state,*” Phys. Rev. Lett. **122** no. 23, (2019) 232001, [1904.00081].
- [10] **ATLAS** Collaboration, G. Aad *et al.*, “*Observation of a B_c^{*+} meson with the ATLAS detector,*” [2605.16228].
- [11] **LHCb** Collaboration, R. Aaij *et al.*, “*Observation of Orbitally Excited B_c^+ States,*” Phys. Rev. Lett. **135** no. 23, (2025) 231902, [2507.02149].
- [12] **LHCb** Collaboration, R. Aaij *et al.*, “*Study of $B_c(1P)^+$ states in the $B_c^+\gamma$ mass spectrum,*” Phys. Rev. D **112** no. 11, (2025) 112003, [2507.02142].
- [13] S. S. Gershtein, V. V. Kiselev, A. K. Likhoded, and A. V. Tkabladze, “ *B_c spectroscopy,*” Phys. Rev. D **51** (1995) 3613–3627, [hep-ph/9406339].
- [14] S. N. Gupta and J. M. Johnson, “ *B_c spectroscopy in a quantum chromodynamic potential model,*” Phys. Rev. D **53** (1996) 312–314, [hep-ph/9511267].
- [15] L. P. Fulcher, “*Phenomenological predictions of the properties of the B_c system,*” Phys. Rev. D **60** (1999) 074006, [hep-ph/9806444].
- [16] D. Ebert, R. N. Faustov, and V. O. Galkin, “*Properties of heavy quarkonia and B_c mesons in the relativistic quark model,*” Phys. Rev. D **67** (2003) 014027, [hep-ph/0210381].
- [17] Q. Li, M.-S. Liu, L.-S. Lu, Q.-F. Lü, L.-C. Gui, and X.-H. Zhong, “*Excited bottom-charmed mesons in a nonrelativistic quark model,*” Phys. Rev. D **99** no. 9, (2019) 096020, [1903.11927].
- [18] G.-L. Wang, T. Wang, Q. Li, and C.-H. Chang, “*The mass spectrum and wave functions of the B_c system,*” JHEP **05** (2022) 006, [2201.02318].
- [19] T.-y. Li, L. Tang, Z.-y. Fang, C.-h. Wang, C.-q. Pang, and X.-Y. Wang, “*Higher states of the B_c meson family,*” Phys. Rev. D **108** no. 3, (2023) 034019, [2204.14258].
- [20] X.-J. Li, Y.-S. Li, F.-L. Wang, and X. Liu, “*Spectroscopic survey of higher-lying states of B_c meson family,*” Eur. Phys. J. C **83** no. 11, (2023) 1080, [2308.07206].
- [21] W. Hao and R. Zhu, “*Beauty-charm meson family with coupled channel effects and their strong decays,*” Chin. Phys. C **48** no. 12, (2024) 123101, [2402.18898].

- [22] Z.-G. Wang, “*Analysis of the vector and axialvector B_c mesons with QCD sum rules,*” Eur. Phys. J. A **49** (2013) 131, [1203.6252].
- [23] T. M. Aliev, S. Bilmis, and M. Savci, “*Mixing angle between 3P_1 and 1P_1 states in heavy axial vector mesons within the QCD sum rules framework,*” Phys. Rev. D **111** no. 1, (2025) 014005, [2408.08014].
- [24] R. Mertig, M. Bohm, and A. Denner, “*Feyn Calc: Computer-algebraic calculation of Feynman amplitudes,*” Comput. Phys. Commun. **64** (1991) 345–359.
- [25] V. Shtabovenko, R. Mertig, and F. Orellana, “*New Developments in FeynCalc 9.0,*” Comput. Phys. Commun. **207** (2016) 432–444, [1601.01167].
- [26] V. Shtabovenko, R. Mertig, and F. Orellana, “*FeynCalc 9.3: New features and improvements,*” Comput. Phys. Commun. **256** (2020) 107478, [2001.04407].
- [27] M. A. Shifman, A. I. Vainshtein, and V. I. Zakharov, “*QCD and Resonance Physics. Theoretical Foundations,*” Nucl. Phys. B **147** (1979) 385–447.
- [28] M. A. Shifman, A. I. Vainshtein, and V. I. Zakharov, “*QCD and Resonance Physics: Applications,*” Nucl. Phys. B **147** (1979) 448–518.
- [29] L. J. Reinders, H. Rubinstein, and S. Yazaki, “*Hadron Properties from QCD Sum Rules,*” Phys. Rept. **127** (1985) 1.
- [30] P. Colangelo and A. Khodjamirian, “*QCD sum rules, a modern perspective,*” [hep-ph/0010175].
- [31] W. Chen, Z.-X. Cai, and S.-L. Zhu, “*Masses of the tensor mesons with $J^P = 2^-$,*” Nucl. Phys. B **887** (2014) 201–215.
- [32] **Particle Data Group** Collaboration, F. Takahashi *et al.*, “*Review of Particle Physics,*” Int. J. Mod. Phys. A **41** (2026) 2630011.
- [33] S. Narison, “*Modern status of heavy quark sum rules in QCD,*” Nucl. Part. Phys. Proc. **312-317** (2021) 87–91, [2101.12579].
- [34] E. Costa i Reina, N. Gubernari, and Z. Wüthrich, “*Decay constants of B_c -mesons with vector and tensor currents,*” [2606.25733].